Modeling of Humidification in Comsol Multiphysics 4.4

Indrajit Wadgaonkar*[1] and Suresh Arikapudi[1]
[1]Tata Motors Ltd. Pimpri, Pune, India, 411018.
*Corresponding author: Indrajit Wadgaonkar, Tata Motors Ltd., Pimpri, Pune, India, 411018, wadgaonkar.indrajit@tatamotors.com

Abstract: Humidification is a complex phenomenon including multiphase flow along with heat and mass transfer. Further the presence of discontinuous phase in the form of water droplets poses even greater a challenge.
In the following study Comsol Multiphysics 4.4 was used to simulate evaporation of water droplets in a stream of heated air. This was a precursor to the modeling of a humidifier, which is used to humidify the air supplied to fuel cell stack. Since the percentage of water droplets was relative low, particle tracing method was used for the simulation. Source terms were added to model evaporation of water droplets due to the heat transfer from surrounding air. However Comsol solves particle tracing in Lagrangian frame and particle variables cannot be passed to air phase, which is solved in Eulerian frame, and vice versa. To circumvent this, a system of PDE's was defined. To remove the limitation on the overall time step of the simulation due to the source term in the energy equation, it was assumed that particle evaporation has no effect on the air temperature. Motion of water droplets in a heated air stream, across a straight channel along with evaporation was modeled and the motion of generated water vapor was tracked. Generated water vapor eventually converged to a parabolic profile as expected for a laminar flow through channel. The rate of evaporation increased with increase in temperature of inlet air while for the range of particle diameters studied it varied to lesser degree. Both, lower and higher velocities of inlet air were found to dampen the rate of evaporation. There is an optimum velocity for maximum evaporation based on the inlet air temperature, channel dimensions etc.

Keywords: Humidification, Comsol.

1. Introduction

Humidifiers have become key components in a variety of applications ranging from air conditioning to fuel cells. Most often humidifiers rely upon evaporation of water droplets which presents a complex heat and mass transfer problem. Hence it is desirous to model the humidification process through Computational Fluid Dynamics (CFD) to gain an insight into aspects like efficiency of evaporation, distribution of evaporated vapor etc. In this study we model the humidification of air in a straight channel flow due to the evaporation of water drops introduced at one end. The simulation domain is given in Fig. 1. As with all problems involving heat and mass transfer convergence requires critical solver settings. Although the application is pretty common and there would be lot of CFD studies in the area, the authors have not referred to any of those since the underlying physics is well defined. Only the expression for rate of mass transfer at the surface of the droplet is taken from [1,2].

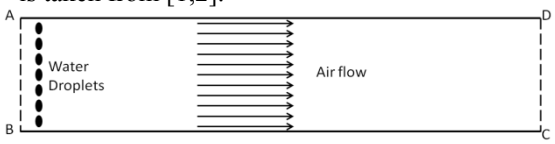

Figure 1. Simulation domain used in the study.

Effect of inlet air temperature, inlet air velocity and the diameter of inserted particles was studied. Along with, the rate of evaporation for laminar flow as compared to turbulent flow was studied. Although, the contours of water vapor concentration represent physical trends; they need to be validated with experiments.

2. Governing equations

The air flow is governed by the Navier Stokes equations. However source terms must be added to the continuity and the energy equations due to the evaporation of water droplets. It is assumed that the presence and evaporation of water droplets has no significant effect on the momentum of air.
The continuity equation is given as:

$$\frac{\partial \rho}{\partial t} + \nabla.(\rho u) = \Gamma(T_p)\dot{m} \qquad (1)$$

Momentum conservation and Energy conservation respectively are:

$$\frac{\partial(\rho u)}{\partial t} + \nabla.(\rho uu) = -\nabla P + \nabla.\left(\mu(\nabla u + \nabla u^T)\right) + F_g \quad (2)$$

$$\frac{\partial(\rho C_p T)}{\partial t} + \nabla.\left(\rho C_p Tu\right) = \nabla.\left(k(\nabla T)\right) - \Gamma(T_p)\left(\nabla.\left(D(\nabla c)\right)M_w h_i + \dot{m}H_e\right) \quad (3)$$

here, u is the velocity vector of air, ρ is the density of air, $\Gamma(T_p)$ is the step function defined below based on the particle temperature T_p , $\dot{m}$ is the rate of evaporation whose expression is taken from [1], P is the pressure field in air,μ is the dynamic viscosity of air and F_g is the applied external force eg. Gravity, D is the diffusion coefficient of water vapor in air which could be constant or calculated from local temperature and pressure conditions, c is the local concentration of water vapor, H_e is the latent heat of evaporation given by $H_e = 2.672.10^5\,(T_{water,cr} - T)^{0.38}$, k is the thermal conductivity of air, C_p is the heat capacity of air, h_i is the enthalpy of diffused vapor and M_w is the molecular weight of water vapor.

The diffusion of water vapor formed is tracked by a transport equation for water vapor given as,

$$\frac{\partial(c)}{\partial t} + \nabla.(cu) = \nabla.\left(D(\nabla c)\right) + \Gamma(T_p)\frac{\dot{m}}{M_w} \quad (4)$$

here, c and D have meaning s as explained above. The motion of water droplets is tracked by the following equation:

$$\frac{\partial v_p}{\partial t} = F_D(u - v_p) \quad (5)$$

where,

$$F_D = \frac{18\mu}{\rho_p d_p^2}\frac{C_d Re_d}{24}; Re_d = \frac{\rho|u - v_p|d_p}{\mu} \quad (6)$$

here C_d is the drag coefficient, d_p is the droplet diameter, v_p is the droplet velocity and ρ_p is the droplet density. The droplet temperature is obtained by the solution of the following equation:

$$m\tilde{C}_p\frac{dT_p}{dt} = hA_p(T_\infty - T_p) + \epsilon_p A_p\sigma(T_\infty^4 - T_p^4) + \Gamma(T_p)\dot{m}H_e Volume_{cell} \quad (7)$$

here $\tilde{C}_p$ is the heat capacity of the droplet, A_p is its surface area and ϵ_p its emissivity, T_∞ is the ambient temperature. The heat transfer coefficient, between the water droplet and surrounding air ,h is given from the following correlation,

$$Nu = \frac{h d_p}{k_{air}} = 2.0 + 0.6Re_d^{1/2}Pr^{1/3} \quad (8)$$

Here, Nu is the Nusselt number while Pr is the Prandtl number based on the properties of air.

The diameter of the water droplet changes as evaporation occurs and it is necessary to update it since it affects the evaporation rate. The updated diameter is given as,

$$d_{p,new} = d_{p,old} - \frac{\dot{m}d_{p,old}}{3m_{old}} \quad (9)$$

Since evaporation occurs only when the droplet temperature exceeds the saturation temperature, T_{sat} , $\Gamma(T_p)$ is a Heaviside function defined as,

$$\Gamma(T_p) = H(T_p - T_{sat}) \quad (10)$$

The expression for the rate of evaporation is ,

$$\dot{m} = \frac{N_i A_p M_{vapor}}{Volume_{element}} \quad (11)$$

Here, A_p is the surface area of the droplet given by $A_p = \pi d_p^2$, while N_i is the molar flux of water vapor leaving the droplet, which is given as:

$$N_i = k_c(c_s - c) \quad (12)$$

c is the concentration of water given by the solution of eq.(4) while c_s is the concentration of water vapor at the surface of the droplet. Assuming the pressure at the droplet surface to be equal to the saturation pressure at temperature T_p, c_s is given as,

$$c_s = \frac{p_{water}^{sat}(T_p)}{RT_p} \quad (13)$$

R is the universal gas constant and $P_{sat}(T_p)$ is either specified or calculated from the semi-empirical Antoine equation as,

$$P_{water}^{sat} = 100.10^{A-\frac{B}{C+(T_p-273.15)}} \quad (14)$$

A,B and C are constants. k_c is the mass transfer coefficient which is obtained by the Sherwood number correlation [1,2] as,

$$Sh = \frac{k_c d_p}{D} = 2.0 + 0.6 Re_d^{1/2} Sc^{1/3} \quad (15)$$

D is the diffusion coefficient of vapor in air and Re_d is the Reynolds number based on the droplet diameter, as earlier. Sc is the Schmidt number, $\frac{\mu_{air}}{\rho_{air} D}$.

2.1 Initial conditions

All the variables were identically set to zero. At boundary AB, 5 particles, each with a mass of 1e-9 kg and temperature of 98 deg C were inserted at the beginning of the simulation.

2.2 Boundary conditions

Following were the boundary conditions:

1) AB- Velocity inlet with velocity ramped up from 0 m/s to 0.2 m/s over a time interval of 0.2 s by a ramp function. Inlet temperature was specified to be 500 K.
2) BC and AD –Wall with No slip; for turbulence these change to standard wall function boundary conditions.
3) CD-Pressure outlet
4) For transport of water vapor concentration no flux boundary condition was applied on all boundaries.

3. Implementation in COMSOL Multiphysics

To implement this model in Comsol Multiphysics 4.4 the CFD module in conjunction with the particle tracing module, to track the water droplets, was used. Source terms can be added to the equations in Comsol Multiphysics as weak contributions with the help of test functions. However the water droplets tracked by particle tracing and the associated variables are calculated in Lagrangian frame of reference while the air flow and the associated variables are calculated in the Eulerian frame of reference. As seen from eqs. (1-15) there is a strong coupling between the particle tracing variables and air flow variables. Comsol Multiphysics 4.4 did not allow for passing of variables between these two reference frames and that posed a serious problem. To circumvent it two separate partial differential equations were defined for the source terms in the energy equation (eq.3) and the species transport equation (eq.4) from the general pde interface in Comsol Multuphysics 4.4 as follows:

$$e_a \frac{\partial^2}{\partial t^2}\begin{bmatrix} u1 \\ v1 \end{bmatrix} + d_a \frac{\partial}{\partial t}\begin{bmatrix} u1 \\ v1 \end{bmatrix} + \nabla . \Gamma = \begin{bmatrix} S1 \\ S2 \end{bmatrix} \quad (16)$$

Here, $e_a = d_a = 0$, while the conservative flux, $= \begin{bmatrix} 0 \\ 0 \end{bmatrix}$. The source terms on the right hand side are set to,

$$\begin{bmatrix} S1 \\ S2 \end{bmatrix} = \begin{bmatrix} -u1 \\ -v1 \end{bmatrix} \quad (17)$$

u1 and v1 would contain the source terms for eq.(3) and eq.(4) respectively. The basic idea was to distribute the particle variables onto the neighboring nodes which can be utilized by the equations in the Eulerian frame (eq.(4)). The calculation of properties based on the concentration would realize the effects obtained from the continuity source terms. The final form of weak contributions to species transport equation and energy equation respectively, were:

$$\text{test}(u1) * \text{fpt.Rp} * (\text{fpt.fs} == 1)/(\text{Molwt} * \text{meshvol}) \quad (18)$$

$$\text{test}(-v1) * (\text{fpt.fs} == 1) * \left(\left(-42000 * \left(\frac{1}{\text{meshvol}}\right) * fpt.Rp * (\text{fpt.fs} == 1)\right) + \text{chds.Dav\_c} * (\text{cxx} + \text{cyy}) * \text{Evap}\left(\text{Tp}\left[\frac{1}{\text{K}}\right] - \text{Tvap}\left[\frac{1}{\text{K}}\right]\right) * \text{Molwt} * \text{nitf.Cp} * \text{T2} * \left(\frac{1}{\text{meshvol}}\right) * (\text{fpt.fs} == 1)\right) \quad (19)$$

The accretion rate given by fpt.Rp was defined as follows:

$$\text{fpt.Rp} = -\text{Evap}(\text{Tp}[1/\text{K}] - \text{Tvap}[1/\text{K}]) * \text{kc} * \text{Adrop} * (\text{Psat}/8.314[\text{J/mol/K}]/(\text{Tp} + \text{eps}) - \text{c}) * \text{Molwt} \quad (20)$$

No change was made in the Continuity, Flow Momentum and the particle momentum equations. Thus, finally we have a system of nine coupled partial differential equations to be solved.

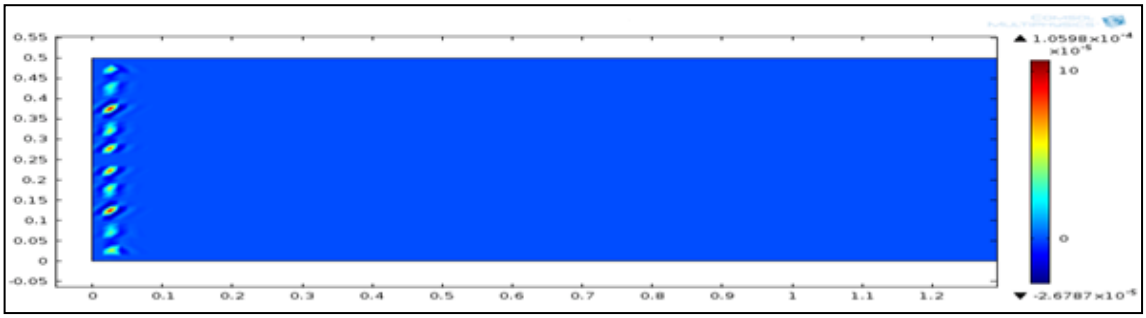

Figure 2. Contours of vapor inside the channel with energy source term . Evaporation occurs as indicated by change in surface concentration; however simulation time is very low as compared to computational time.

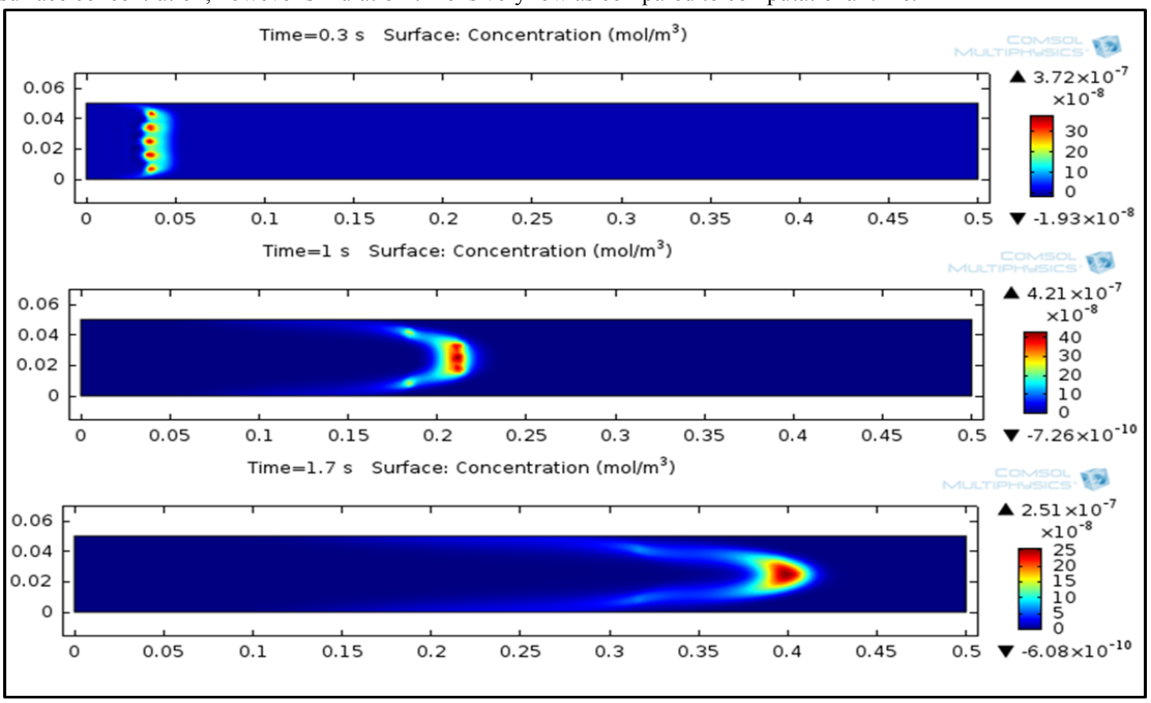

Figure 3. Contours of vapor inside the channel without energy source term. Evaporation occurs as indicated by change in surface concentration; formed water vapor takes up parabolic velocity profile of channel air.

4. Results and Discussion

The system of equations is extremely stiff and the occurrence of evaporation makes convergence even more difficult. The solver was found to be restricted to the time steps of as low as 1e-9 increasing the total computational time beyond feasible limits. After about running the simulation for a day on a system with 8 GB ram there was no significant evaporation or displacement of water droplets as seen from Fig.2. It was observed that the source terms in the energy equation were restricting the time steps to such low values. At this point an approximation was introduced that the evaporation did not have any effect on the temperature of the air flow in the channel. Given the fact that amount of water droplets inserted

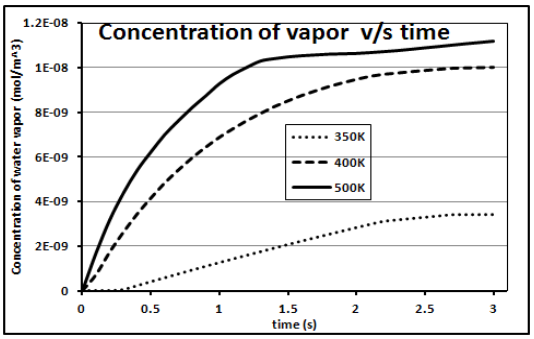

Figure 4.Water vapor concentration v/s time for different temperatures of inlet air

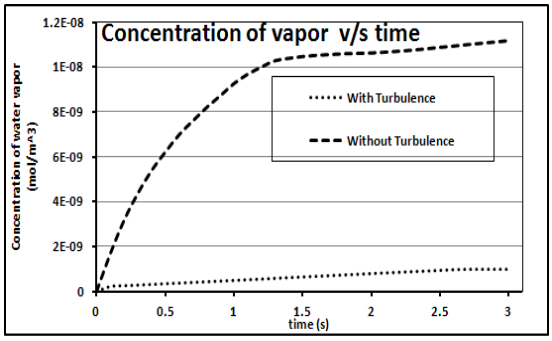

Figure 5.Water vapor concentration v/s time with and without turbulence.

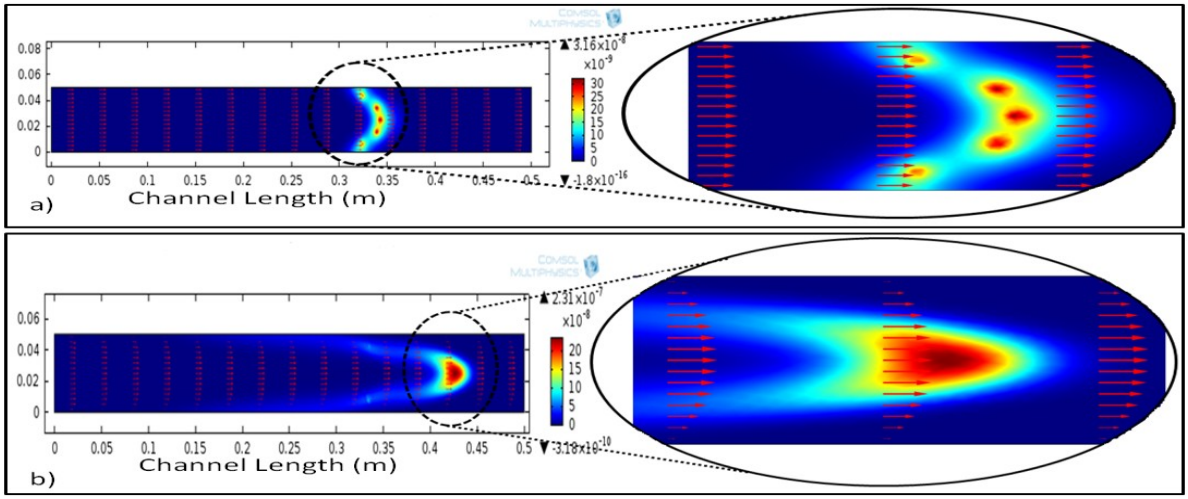

Figure 6. Water Vapor concentration a) with turbulence and b) without turbulence (laminar flow). Enlarged images on the right hand side show the velocity profiles and details of concentration contours.

Temperature (K)	Evaporation initiation length (m)
350	0.03
400	0.00115
500	0.001

Table1.The length of channel after which evaporation starts for different temperatures of inlet air

	Residence time of particles in the channel (s)
With Turbulence	2.5
Without Turbulence	2

Table 2. Residence time of particles in the channel.

was less than 10% by weight, this approximation seems plausible for the case studied. As such the source term in the energy equation (eq.3) was eliminated. This increased the time step of the simulation to 1e-3s thereby drastically reducing the total computational time. Fig.3 shows the contours of water vapor with time. As observed, the contours eventually the water vapor takes up parabolic profile which is characteristic of laminar flow. This is expected since the water vapor formed should eventually align with the air flow in the channel which is laminar. Figure 4 shows the variation of water vapor concentration with time for different temperatures of inlet air.

As expected, with higher inlet air temperatures the rate of evaporation increases. Also with increase in inlet air temperature, evaporation sets of early as seen from Table 1.Figure 5 shows the variation of water vapor concentration with turbulence. As seen from Figure 6, the velocity profiles are no longer parabolic resulting in better distribution of water vapor across the cross section area. However, with turbulence evaporation rate is very low as seen from Figure 5. As seen from Table 2, the residence time of particles inside the channel is higher with turbulence which is as expected.

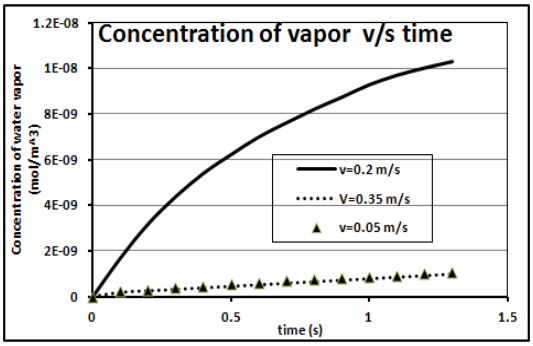

Figure 7.Water vapor concentration different velocities of inlet air.

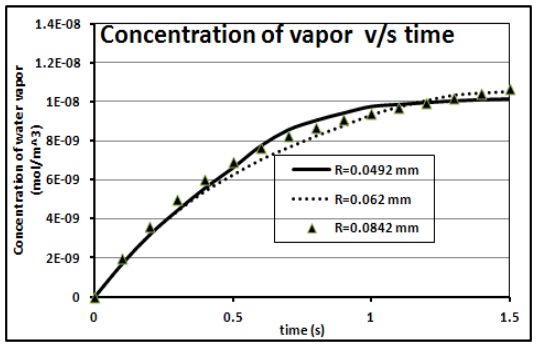

Figure 8. Water vapor concentration for different radii of inserted particles.

Figure 7 shows the variation of water vapor concentration with time for different velocities of inlet air. Higher velocities are expected to decrease the residence time thereby decreasing the evaporation of water droplets which is evident from Figure 7 for velocities of 0.2 m/s and 0.35 m/s. However as seen from Figure 6, for lower velocities of 0.05 m/s the rate of evaporation drops. For extremely low inlet velocities the drag on the particles reduces thereby reducing particle velocity which would lead to reduced mass transfer coefficient. Hence there would be an optimum velocity of inlet air for maximum evaporation as suggested by Figure 7. Next we investigated the effect of diameter of particles on the evaporation rate. The radius of the water droplets inserted was changed while keeping the cumulative mass of water droplets constant by adjusting the number of droplets inserted. As seen from Figure 8, for the range of diameters studied the effect was not very pronounced.

5. Conclusions

Although evaporation induced by convective heat transfer is an inherently difficult problem for computational fluid dynamics analysis, it was modeled with the help of Comsol Multiphysics. The transient phenomenon, of water vapor formation and the transport of the vapor so formed was captured well. The increase in surface concentration of the vapor across the channel and the parabolic profile taken up by the formed vapor proves that humidification has been modeled satisfactorily. It was observed that with higher temperature of inlet air, the rate of evaporation increased. Higher temperature of inlet air would lead to higher particle temperature thereby increasing evaporation. However the rate of evaporation was found to decrease when turbulence was added to the model. This needs further investigation since turbulence was expected to enhance heat transfer. For the range of inlet particle diameters studied the rate of evaporation did not vary much. However it was found that too high or too low velocities lead to a decreased rate of evaporation. Higher velocities decrease the residence time of the droplets in the channel thereby decreasing evaporation, whereas lower velocities decrease particle Reynolds's number thereby decreasing mass transfer. Hence for a particular channel geometry there has to be an optimum inlet air velocity for maximum evaporation. Finally, the model can be extended to include complex geometries to suit real life applications of humidifiers and give a quantitative estimate of various performance parameters of the humidifiers like residence time for complete humidification, distribution characteristics of vapor formed etc.

6. References

1. W. E. Ranz and W. R. Marshall, Jr., Evaporation from Drops, Part I., Chem. Eng. Prog., 48(3), 141-146 (1952)
2. W. E. Ranz and W. R. Marshall, Jr., Evaporation from Drops, Part II., *Chem. Eng. Prog.*, ***48(4)***, 173-180 (1952)

7. Acknowledgements

The study was carried out with the support of Advanced Engineering Department at Tata Motors Ltd., Pune.